Liquid Crystals
Publication details, including instructions for authors and subscription information:
http://www.informaworld.com/smpp/title~content=t713926090

Liquid crystal comb polymer with polar mesogenic and aliphatic side groups I. Preparation and structural properties

B. Gallot; P. Allia; P. Taverna; L. Trossi; C. Cucinelli; S. Ponti

To cite this Article Gallot, B. , Allia, P. , Taverna, P. , Trossi, L. , Cucinelli, C. and Ponti, S.(2002) 'Liquid crystal comb polymer with polar mesogenic and aliphatic side groups I. Preparation and structural properties', Liquid Crystals, 29: 3, 397 — 404

To link to this Article: DOI: 10.1080/02678290110104603

URL: http://dx.doi.org/10.1080/02678290110104603

LIQUID CRYSTALS, 2002, VOL. 29, NO. 3, 397–404

Liquid crystal comb polymer with polar mesogenic and aliphatic side groups

I. Preparation and structural properties

B. GALLOT
CNRS, Laboratoire des Matériaux Organiques à Propriétés Spécifiques,
69390 Vernaison, France

P. ALLIA*, P. TAVERNA, L. TROSSI
INFM, UdR Torino Politecnico, I-10129 Torino, Italy

C. CUCINELLI and S. PONTI
Dipartimento di Fisica, Politecnico di Torino, I-10129 Torino, Italy

(*Received 29 June 2001; accepted 20 September 2001*)

A liquid crystal comb polymer of potential interest for electro-optical applications has been synthesized and characterized. The polymer has a polyacrylamide main chain and two different types of side group, built up of 4′-undecanoyloxy-4-cyanobiphenyl groups (68 mol %) and of shorter aliphatic groups (32 mol %). The two types of side group occur randomly along the polymer's main chain. The preparation steps and the liquid crystalline structure of the resulting copolymer are compared with those of a homopolymer whose side groups (built up of 4′-undecanoyloxy-4-cyanobiphenyl groups) are all identical. X-ray diffraction shows that the polymers display different mesophases over different temperature ranges. However, the homopolymer exhibits two smectic phases (SmC_2 and SmA_2), while the new copolymer exhibits a SmC_2 phase and a nematic mesophase at higher temperature. The mesophase thermal stability of the copolymer is significantly lower than that of the homopolymer.

1. Introduction

Liquid crystal comb polymers are a class of mesomorphic materials with distinctive physical properties and prospective applications in electro-optical devices. These systems have been extensively studied both experimentally and theoretically [1–8]. Comb polymers are usually composed of rigid mesogenic units linked to a polymeric backbone by flexible spacers, such as methylene groups. Comb polymers are usually more stable and stiffer than many other liquid crystalline systems, so that they can be viewed as potential passive elements in certain applications, e.g. as orienting substrates for softer liquid crystals in electro-optical cells. On the other hand, these materials may be made of monomers containing strongly polar groups, so that they can be of use as active elements in electro-optical devices, exploiting their response to an applied electrical field [9, 10]. Comb polymers are interesting because their physical properties, including stability and dielectric behaviour, can be tuned by suitably choosing the types of constituent monomers. Recently, comb polymers corresponding to the formula:

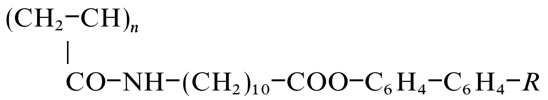

$$\begin{array}{l}(CH_2{-}CH)_n\\ \quad\;\; |\\ \quad\;\; CO{-}NH{-}(CH_2)_{10}{-}COO{-}C_6H_4{-}C_6H_4{-}R\end{array}$$

have been synthesized and characterized [11, 12]. The letter R in the chemical formula indicates any substituent linked to the biphenyl-based mesogenic unit of the side group. So far, the following substituents in the biphenyl core have been considered: H, CN, $OCH_2CH(CH_3)C_2H_5$ [12–15]. These substituents substantially differ in mass and polar properties. However, a really significant influence of the electrical field on their optical properties has never been observed even in the case of the material containing the highly polar CN group. Such a puzzling circumstance is possibly related to the electrostatic interaction among polar groups, inhibiting the reorienting effect of the field. In any case, the price paid for having a stiff liquid crystalline material is a nearly complete lack of macroscopic response to an electrical field. A new type of comb polymer has been designed to overcome this difficulty. Its chemical nature, preparation, and

---

*Author for correspondence; e-mail: allia@ien.it

Liquid Crystals ISSN 0267-8292 print/ISSN 1366-5855 online © 2002 Taylor & Francis Ltd
http://www.tandf.co.uk/journals
DOI: 10.1080/02678290110104603

structural properties are discussed in the present paper. Complementary optical measurements, mainly devoted to a study of the thermal noise of scattered light, will be presented and discussed in a second paper (Part II). The combined analysis of static and dynamical properties will allow us to draw a rather complete picture of the new polymer.

2. Experimental

Dicyclohexylcarbodiimide (DCC), pyrollidinopyridine (PPY), 11-aminoundecanoic acid, 4′-hydroxy-4-biphenylcarbonitrile from Aldrich, and *n*-decylamine were used as received. α,α′-Azobisisobutyronitrile (AIBN, purity 99% from Merck) was recrystallized before use. Solvents were purified by classical methods.

2.1. *Synthesis of the monomers*

2.1.1. *Cyanobiphenyl monomer (**III**)*

In a first step, 11 g (196 mmol) of KOH were dissolved in 300 ml of water, then 10 g (50 mmol) of 11-aminoundecanoic acid (**I**) were added and the solution was cooled to 0°C; 8 ml (98 mmol) of acryloyl chloride were then added drop-wise with agitation. After 4 h of reaction at 0°C, 1M CHl was added until a pH = 2 was obtained; the precipitate formed was filtered off, washed with cold HCl and dried under vacuum. The precipitate was dissolved in 250 ml of ethyl acetate and washed with slightly acidified water. The organic phase was dried over $MgSO_4$ and evaporated (yield 84%). TLC: $R_f = 0.46$, eluant $CHCl_3$/MeOH (10/1). FTIR (Nicolet 20SX), cm^{-1}: 3305, 1650, 1530 (amide), 2920 (aliphatic chain), 1695 (carboxyl group), 1625 (C=C). ^1H NMR, 250 MHz (MeOD, TMS) ppm: 1.32 (m, 12H), 1.56 (m, 4H), 2.7 (t, 2H), 3.2 (m, 2H), 5.3 and 5.62 (dd, 1H), 6.2 (d, 2H).

In the second step, a solution of 6.55 g (25.7 mmol) of 11-acryloylamidoundecanoic acid in 125 ml of dry CH_2Cl_2 was degassed under an inert atmosphere. Then 5.1 g (25.7 mmol) of 4′-hydroxy-4-biphenylcarbonitrile and 3.8 g (25.7 mmol) of PPY were added. The solution was cooled to 0°C and a solution of 5.85 g (25.7 mmol) of DCC in 20 ml of anhydrous CH_2Cl_2 was added drop-wise. After 20 min at 0°C and 72 h at r.t., the solution was filtered to remove the precipitate of DCU; the filtrate was first washed with 0.5M HCl and subsequently with saturated aqueous $NaHCO_3$; the organic solution was dried over $MgSO_4$ and evaporated. The precipitate was recrystallized from acetonitrile at 64°C; on cooling it was filtered off, washed with acetonitrile and dried under vacuum (yield 83%). TLC: $R_f = 0.37$, eluant AcOEt/C_6H_{12}/$CHCl_3$ (3/3/5). FTIR (Nicolet 20SX), cm^{-1}: 3295, 1653, 1542 (amide), 2921, 2851 (aliphatic chain), 1748 (ester) 1625 (vinyl), 2227 (CN). ^1H NMR, 250 MHz ($CDCl_3$, TMS) ppm: 7.8–7.1 (H aromatic), 6.0–6.3 (Hb and Hc), 5.6 (Ha), 5.85 (–NH–), 3.3 (t, 1H), 2.58 (t, H10), 1.78 (m, 2H), 1.55 (m, 9H). The ^1H NMR spectrum of this monomer is reported in figure 1.

2.1.2. *Decylacryloylamide monomer (**IIIb**)*

10 ml of *n*-decylamine were dissolved in a mixture of 400 ml of water containing 4% of KOH and 150 ml of methanol. Then the solution was cooled to 4°C and 10 ml of distilled acryloyl chloride were added drop-wise

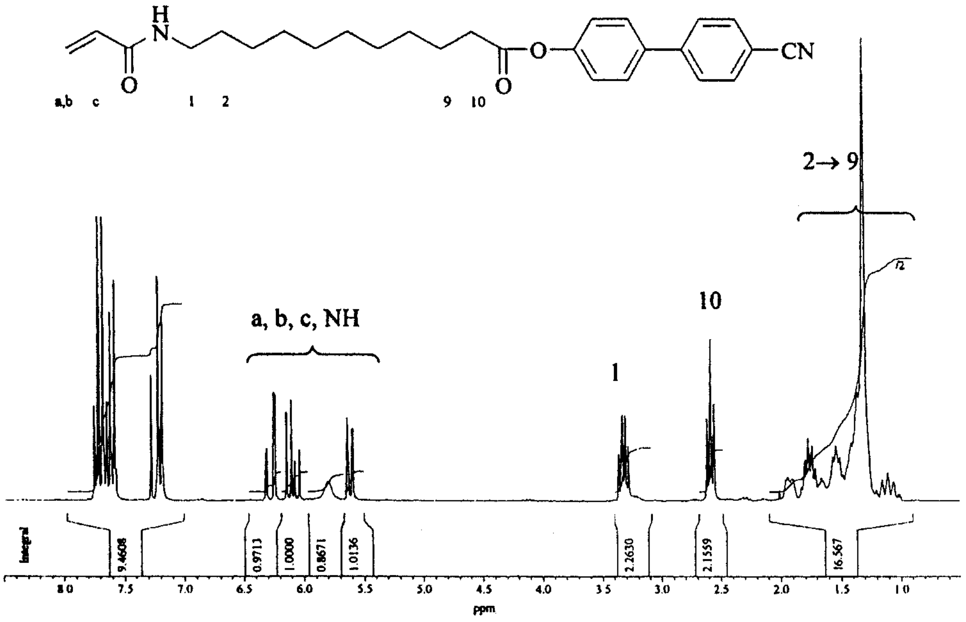

Figure 1. ^1H NMR spectrum of the monomer **III** in $CDCl_3$.

with agitation. After 12 h at r.t., 6M HCl was added until neutralization, and water was added until completion of precipitation. The precipitate was filtered off, washed first with water, and then several times with a 20% aqueous solution of acetic acid. The monomer was dried at room temperature under vacuum (yield 61%). FTIR (Nicolet 20SX), cm^{-1}: 3295, 1653, 1542 (amide), 2921, 2851 (aliphatic chain), 1625 (vinyl). ^{1}H NMR 250 MHz ($CDCl_3$, TMS) ppm: 6.0–6.3 (Hb and Hc), 5.6 (Ha), 5.65 (–NH–), 1.25 (t, H10), 1.5 (m, 9H), 1.25 (t, 16H), 0.9 (3H). The ^{1}H NMR spectrum of this second monomer is reported in figure 2.

2.2. *Polymerization*

2 g of Cyanobiphenyl monomer (**III**) were dissolved in 10 ml of chloroform, 0.05 g of AIBN were added and the solution was degassed under vacuum. The solution was maintained at 65°C for 150 h under vacuum and with stirring. The polymer was recovered by precipitation in methanol. Copolymers were prepared under similar conditions starting from a solution of the monomers in the desired molar composition.

2.3. *Polymer characterization*

The copolymer was characterized by ^{1}H NMR, 250 MHz ($CDCl_3$, TMS) ppm: 1.3 (m, 16H), 2.6 (t, 2H), 3.3 (m, 2H), 7.1–7.7 (m, 8H aromatic). The composition of the copolymer was determined by ^{1}H NMR from the peaks for the aromatic protons (7.1–7.7) and methyl protons (0.88). The molecular characteristics of the polymer (M_n, M_w and M_w/M_n) were determined by light scattering (Brookhaven) in THF and gel permeation chromatography in THF (PSS gel mixed b columns) using polystyrene calibration.

2.4. *X-ray diffraction*

X-ray diffraction (XRD) experiments were performed on non-oriented samples with two types of camera: Guinier-type and pinhole. The Guinier-type focusing camera, operated under vacuum, was equipped with a bent quartz monochromator (reflection 1 0 1) giving a linear collimation of strictly monochromatic X-rays (CuK_α, $\lambda = 1.54$ Å) and with a device for recording the diffraction patterns from samples at various temperatures between 20 and 200°C with an accuracy of ±1°C. The pinhole camera was specially designed in the laboratory to operate with powders or oriented samples, under vacuum, with a Ni-filtered Cu beam ($\lambda = 1.54$ Å). It was equipped with the same heating device as the Guinier camera. Several exposures were made in order to measure the strongest and the weakest reflections. The reflection intensities were measured through a laboratory-built microdensitometer properly designed to analyse X-ray diagrams provided by linear focusing and through pinhole cameras. Experimental diffraction amplitudes of the different orders of reflections from the smectic layers were corrected by the Lorentz-polarization factor [16] and normalized so that the amplitude of

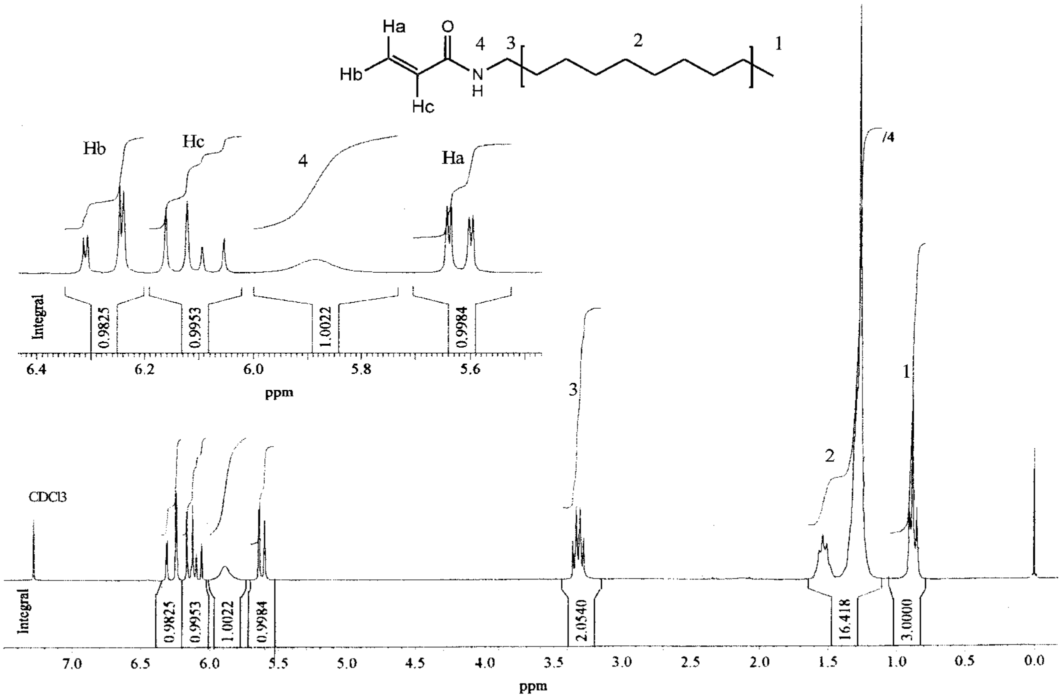

Figure 2. ^{1}H NMR spectrum of the monomer **IIIb** in $CDCl_3$.

the strongest reflection is equal to unity. The following values refer to the first phase of the copolymer: $a_1 = 1$, $a_2 = 0.31$, $a_3 = 0.42$.

3. Results

3.1. *Synthesis of polymers*

The acryloylamidoundecanoyloxybiphenyl monomer **III** was synthesized in 2 steps. In the first, the 11-aminoundecanoic acid **I** was transformed into the polymerizable acid **II** by nucleophilic reaction between acryloyl chloride and the amino group in aqueous KOH solution at basic pH to increase the reactivity. In the second step, the polymerizable acid **II** was esterified by 4′-hydroxy-4-cyanobiphenyl in the presence of a coupling agent DCC and also PPY, which modifies the equilibrium of the reaction by formation of *N*-acyl-pyridiniuin salts, which are more electrophilic and increase both the speed and yield of the reaction [17, 18]:

$$H_2N{-}(CH_2)_{10}{-}COOH\ (\mathbf{I})$$

$$H_2C{=}CH{-}COC1 \quad \downarrow$$

$$H_2C{=}CH{-}CO{-}NH{-}(CH_2)_{10}{-}COOH\ (\mathbf{II})$$

$$HO(C_6H_4C_6H_4)CN \quad \downarrow \quad DCC,\ PPY$$

$$H_2C{=}CH{-}C0{-}NH{-}(CH_2)_{10}{-}COO{-}C_6H_4{-}C_6H_4{-}CN\ (\mathbf{III})$$

The second monomer **IIIb** was synthesized in a single step by action of acryloyl chloride on *n*-decylamine; however, owing to the insolubility of the amine in water, a basic mixture of water and methanol was used as solvent:

$$H_2C{=}CH{-}COCl$$

$$H_2N{-}(CH_2)_9{-}CH_3 \quad \downarrow$$

$$H_2C{=}CH{-}CO{-}NH{-}(CH_2)_9{-}CH_3\ (\mathbf{IIIb})$$

The homopolymerization of the monomer **III** and its copolymerization with the monomer **IIIb** were carried out with AIBN initiator at 65°C under vacuum in chloroform solution, and gave respectively the homopolymer **IV**:

$$-(CH_2{-}CH)\ p-$$

$$CO{-}NH{-}(CH_2)_{10}{-}COO{-}C_6H_4{-}C_6H_4{-}CN\ (\mathbf{IV})$$

and the copolymer **IVb**:

$$-(CH_2{-}CH{-}R_1)_x{-}(CH_2{-}CH{-}R_2)_{(1\text{-}x)}\ (\mathbf{IVb})$$

where:

$$R_1{=}CO{-}NH{-}(CH_2)_{10}{-}COO{-}C_6H_4{-}C_6{-}H_4{-}CN$$

and

$$R_2{=}CO{-}NH{-}(CH_2)_{10}{-}H$$

The molecular characteristics of the homopolymer **IV** were easily determined by light scattering and GPC. A rather high molecular mass ($M_n = 68\,000$ and $M_w = 88\,100$) and a low dispersity ($M_w/M_n = 1.28$) were found. For the copolymer **IVb**, only the molar composition could be determined. The molar composition found by NMR (68.2/31.8) was in good agreement with the composition of the starting monomer solution (70/30). Furthermore, the reactivities of the two monomers are similar (the polymerizable double bond is linked to a long aliphatic chain through an amide bond for both monomers), so the molecular mass of the copolymer is probably similar to that of the homopolymer.

3.2. *Liquid crystal behaviour of the polymers*

3.2.1. *Homopolymer (IV)*

For the homopolymer **IV** two mesophases were found: a bilayer disordered tilted SmC_2 at lower temperatures, followed by a bilayer disordered orthogonal SmA_2 at higher temperatures [13].

3.2.2. *Copolymer (IVb)*

For the copolymer, all X-ray patterns recorded as functions of temperature can be classified in two families corresponding to two different mesophases, as summarized below.

For the first mesophase, at temperatures between room and about 70°C, X-ray diagrams exhibit in the low angle domain three sharp reflections; in the wide angle domain a diffuse band appears (figure 3). The low angle reflections can be indexed as the 0 0 1 reflections of a lamellar structure of thickness $d = 50.5$ Å. The wide angle band at 4.4 Å (figure 3) is typical of a disordered

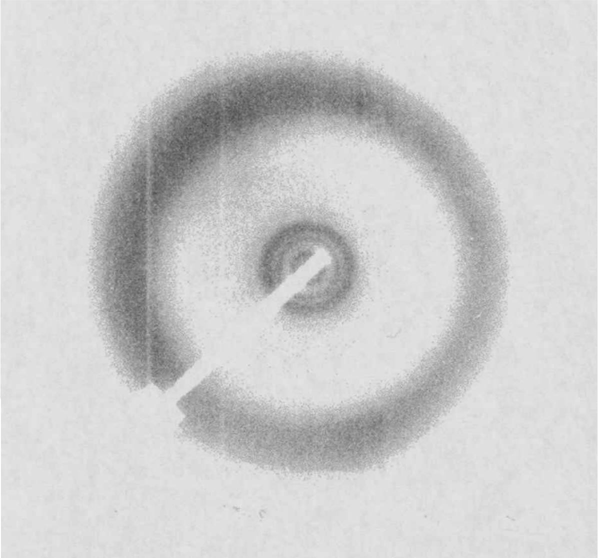

Figure 3. Pinhole camera powder X-ray diagram of the SmC_2 mesophase of the polymer **IV** at room temperature, showing the three small angle sharp reflections and the wide angle diffuse band.

smectic structure (either smectic A or C) [19]. In order to decide between the two possible smectic structures, the thickness d of the smectic layers has been compared with the thickness $d_1 = p + l_1$ (one main chain plus one side chain) and $d_2 = p + 2l_1$ (one main chain plus two side chains) corresponding to a monolayer and a bilayer model, and obtained by measurements with CPK models (with the spacer in the 'all-*trans*' conformation) of the lengths of the repeating units of the copolymer.

We found that $d_1 = 30.5\,\text{Å}$ and $d_2 = 57\,\text{Å}$. As a consequence, the structure, characterized by the intermediate thickness value $d = 50.5\,\text{Å}$, can be either a bilayer tilted SmC_2 structure, with an angle of tilt $\alpha = 28°$ given by $\cos\alpha = d/(p + 2l_1)$, or an interdigitated orthogonal SmA_d.

In principle, two different methods can be adopted to distinguish between the possible liquid crystal structures: the intensity profiles $\rho(z)$ along the z-axis perpendicular to the smectic planes can be derived from the intensities of the low angle reflections of the X-ray diagrams [16]; alternatively, one can try to draw oriented fibres of the polymers. Although we succeeded in drawing oriented fibres for the homopolymer [13], it was impossible to obtain oriented fibres for the copolymer. Consequently, the electron density profiles were derived from the X-ray patterns.

Taking into account the fact that as many mesogenic cores are pointing along the $+z$ and $-z$ axes and that we are measuring only the fluctuations around $\rho(z = 0)$, the average electron density $\rho(z)$ [16, 20] is given by:

$$\rho(z) = \sum_n a_n \cos\left(n\frac{2\pi z}{d}\right). \tag{1}$$

Actually, the intensity of the diffraction orders is being measured, so that the phase information is lost. Owing to the symmetry of the electron density distribution, the phase factor and the structure factor must be 0 or π, so the a_n coefficients are real, but they may be either positive or negative. The phase problem then reduces to choosing the right combinations of sign for a_n ($n = 1, 2, 3$). For instance, $\rho_{+-+}(z)$ will correspond to the combination where a_1 and a_3 are chosen positive, while a_2 is chosen negative. As three orders of diffraction are actually observed, eight combinations of sign for the a_n constants are obtained; that is to say, eight electron density profiles $\rho(z)$, as sketched in figure 4. In order to single out the physically acceptable profile from the entire set, the electron densities of the different parts of the repeating unit of the polymer have been calculated by dividing their number of electrons by their lengths measured using CPK models. The following results were obtained: $9.2\,\mathrm{e\,Å^{-1}}$ for the skeleton, $6.4\,\mathrm{e\,Å^{-1}}$ for the paraffinic spacer; and $8.8\,\mathrm{e\,Å^{-1}}$ for the mesogenic group.

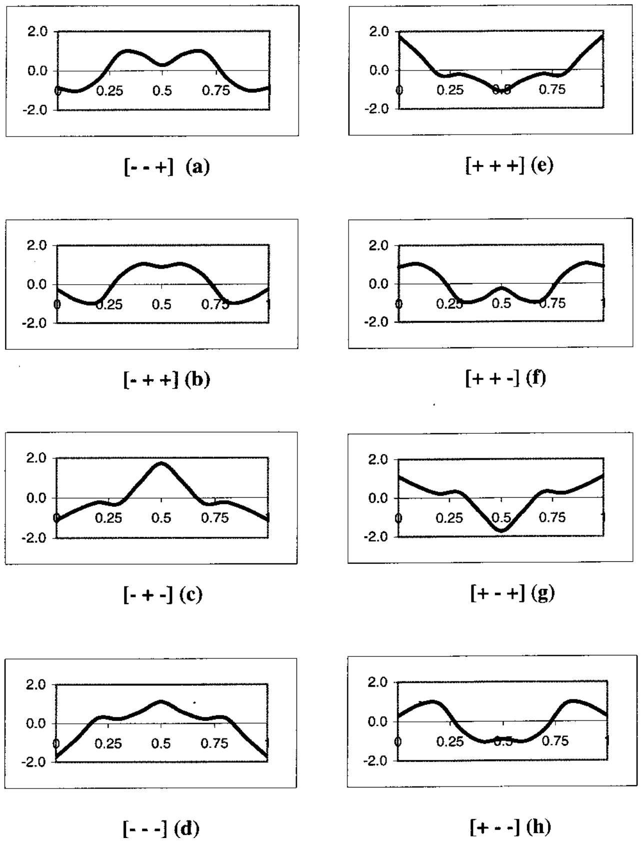

Figure 4. Projections of the electron density profiles corresponding to the eight different sign combinations of the a_n coefficients for the copolymer **IVb** in the SmC_2 phase.

Let us now briefly discuss the expected electron density profiles corresponding to the different liquid crystal structures. In the case of an orthogonal interdigitated structure SmA_d, one should observe a central maximum corresponding to the partly interdigitated mesogenic groups surrounded by two minima (corresponding to the spacers) and two maxima (corresponding to the polymeric skeleton). On the other hand, in the case of a double layer tilted smectic structure SmC_2, one should observe a central minimum surrounded by two maxima (corresponding to the mesogenic cores), two minima (corresponding to the paraffinic spacers), and two additional maxima (corresponding to the polymeric skeleton). Comparing these requirements with the electron density profiles of figure 4, it is concluded that, for the low temperature phase of the copolymer, the four electron density profiles labelled (*e*–*h*) must be rejected, as they exhibit a minimum for the mesogenic cores. The electron density profiles (*c*) and (*d*) must also be rejected, as they exhibit minima for the main chains. Finally, the electron density profiles (*a*) and (*b*), corresponding to ρ_{--+} and to ρ_{-++}, display a central minimum surrounded by maxima for the mesogenic cores, minima for the paraffinic spacers, and maxima for the main chain; as a consequence, they are in agreement with a double layer tilted smectic structure. As no electron density profiles match an interdigitated smectic structure, whereas two profiles match a double layer smectic structure, it can be concluded that the low temperature mesophase of the copolymer is a disordered, double layer, tilted smectic (SmC_2), with a tilt angle $\alpha = 28°$.

For the second mesophase, at temperatures between about 70°C and 100°C, X-ray diagrams exhibit a diffuse band both in the low angle and in the wide angle domains (figure 5). They are typical of a nematic mesophase, as confirmed by polarizing optical microscopy.

3.3. *Effect of temperature*

The presence of two mesophases at low and high temperature is a common feature of both polymers (labelled CP and SP); however, their nature is different. In fact, the SP homopolymer **IV** was previously observed to exhibit two smectic phases: a bilayer tilted smectic phase between r.t. and 95°C, followed by a bilayer orthogonal SmA_2 phase between 95 and 165°C [13]. The CP copolymer **IVb** exhibits instead a bilayer tilted SmC_2 for temperatures lower than about 70°C, followed by nematic phase between about 70 and 100°C. For all smectic arrangements, within the whole temperature range of their existence, the thickness d of the smectic layers remains constant and independent of temperature. The values of the structural parameters found on heating were reversibly obtained on cooling. The structural properties of the CP polymer are compared with those of the SP homopolymer in the table.

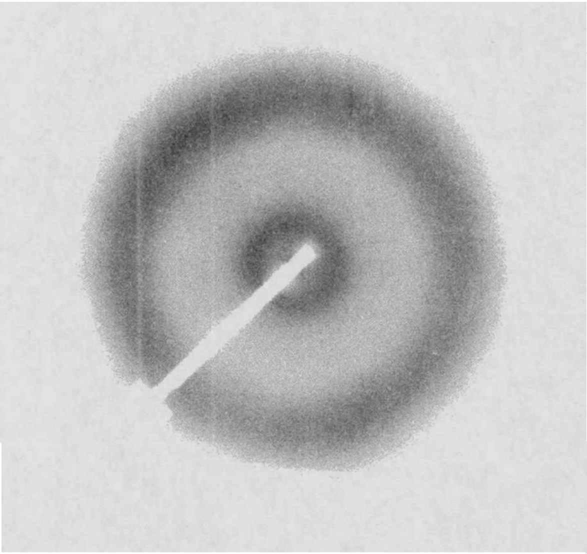

Figure 5. Pinhole camera powder X-ray diagram of the nematic mesophase of polymer **IV** at 110°C, showing the low angle and the wide angle diffuse bands.

3.4. *Polarizing optical microscopy*

The CP copolymer was submitted to polarizing microscopy. A sample was prepared by inserting a solution of the polymer in chloroform between two glass slides by capillary action. A Leitz Laborlux 12 Pol S polarizing microscope was used. The temperature of the sample was increased from r.t. to about 110°C by means of an electrically controlled heater ensuring an overall stability of ±0.1°C. In this way, mesomorphic textures of the sample were observed at different temperatures.

Figure 6 shows the image obtained at $T = 20°C$ by placing the sample between crossed polarizers, with the optical axis of the sample forming an angle of 45° with

Figure 6. Room temperature texture of the CP polymer between crossed polarizers (optical axis at an angle of 45° to the analyser axis).

Table. Structural properties of the liquid crystalline comb polymers SP and CP.

Property	Homopolymer (SP), ref. [13]	Copolymer (CP)
Low temperature mesophase	Disordered SmC_2	Disordered SmC_2
Interlayer distance/Å	51.8	50.5
Angle of tilt/°	24.7	28
Transition temperature/°C	95	72
High temperature mesophase	Disordered SmA_2	Nematic
Interlayer distance/Å	59	—
Angle of tilt/°	0	—
Isotropization temperature/°C	168	102

respect to the analyser axis. A well-defined smectic phase is observed. Observation of a general change of the sample configuration commences at about 74°C (figure 7). This result is in rather good agreement with the XRD data (see above). The transition from the smectic to the nematic phase seems to be complete at about 80°C; the nematic phase appears to be stable up to 85°C, when some melting is observed, as shown in figure 8.

The same transition is also observed by inserting the sample between crossed polarizers, with the optical axis parallel to the analyser axis. Figure 9 shows good extinction of light at room temperature, whereas figure 10 shows the typical birefringence of the nematic phase at 80°C. The start of the melting process is again observed at 86°C; at higher temperatures, the intensity of the transmitted light decreases, as expected for a system submitted to a melting process; a feeble birefringence is however observed up to 104°C, indicating that the sample isotropization takes place over an extended temperature interval.

4. Concluding remarks

The preparation procedures and the static structural properties of two similar comb polymers with polyacrylamide main chain have been compared. The CP copolymer has a mixture of 4′-undecanoyloxy-4-cyanobiphenyl side groups and purely aliphatic side groups, such that the molar content of mesogenic units is reduced to about 68% with respect to the SP homopolymer, which is instead characterized by side groups formed entirely by 4′-undecanoyloxy-4-cyanobiphenyl groups. XRD shows that both comb polymers exhibit two distinct phases, although the low temperature mesophase (SmC_2) is the same for both polymers, while they differ by the nature of the second mesophase. A disordered orthogonal bilayer SmA_2 phase was observed in the homopolymer, while a less ordered nematic phase appears in the copolymer. It can be concluded that partially substituting undecanoyloxycyanobiphenyl groups with aliphatic groups for the polymer side groups brings about not only a lower mesophase thermal stability, but also a looser liquid crystal arrangement at high temperatures. These structural results will be used to support the dynamical description of the CP copolymer obtained through optical measurements, as discussed in Part II [21].

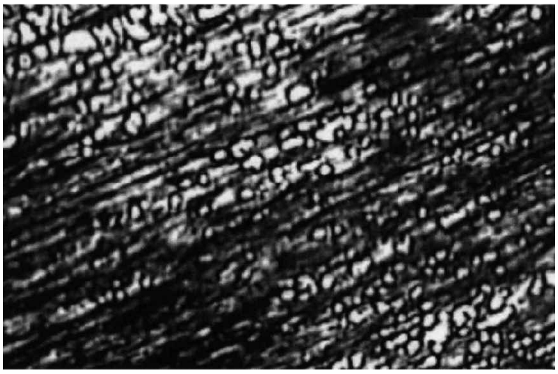
Figure 7. The same as in figure 6 at $T = 80$°C.

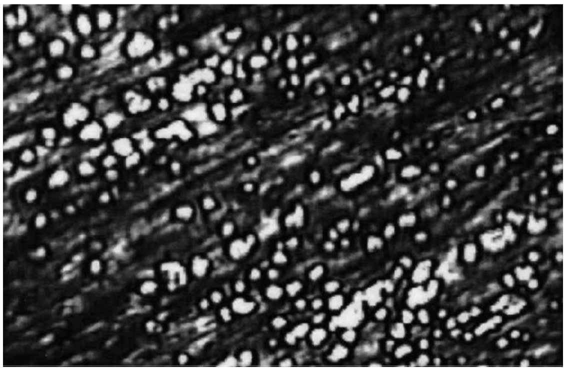
Figure 8. The same as in figure 6 at $T = 85$°C.

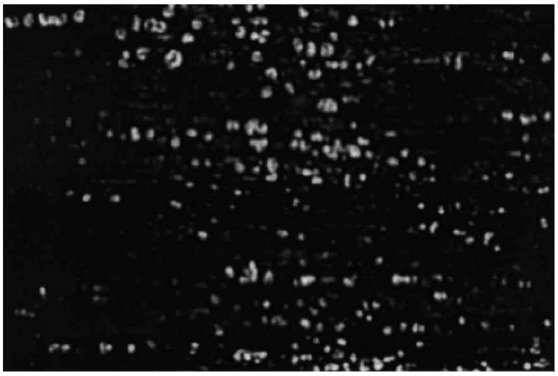
Figure 9. Room temperature image of the CP polymer between crossed polarizers (optical axis parallel to the analyser axis).


Figure 10. The same as in figure 9 at $T = 80$°C.

References

[1] Blumstain, A., 1978, *Liquid Crystalline Order in Polymers* (New York: Academic Press) and references therein.

[2] MATHIAS, L. J., and HERMES, R. E., 1986, *Macromolecules*, **19,** 1536.
[3] MATHIAS, L. J., 1988, *Polym. Commun.*, **29,** 352.
[4] UNAYAMA, S., NAKAJIMA, K., IKEHARA, T., NISHI, T., and TSUKAHARA, Y., 1996, *Jpn. J. appl. Phys.*, **35,** 2280.
[5] YURASOVA, T. A., MCLEISH, T. C. B., and SEMENOV, A. N., 1994, *Macromolecules*, **27,** 7205.
[6] GALLOT, B., and DOUY, A., 1987, *Mol. Cryst. liq. Cryst.*, **153,** 367.
[7] GALLOT, B., and MARCHIN, B., 1989, *Liq. Cryst.*, **5,** 1719.
[8] GALLOT, B., and MARCHIN, B., 1989, *Liq. Cryst.*, **5,** 1729.
[9] MCARDLE, C. B., 1989, *Side Chain Liquid Crystal Polymers* (Blackie), 330–394.
[10] DUBOIS, J. C., 1995, *Polym. Adv. Technol.*, **6,** 10.
[11] SHIBAEV, V. P., PLATE', N. A., SMOLIANSKI, A. L., and VOLOSKOV, A. K., 1989, *Makrmol. Chem.*, **181,** 1393.
[12] GALLOT, B., and MONNET, F., 1996, *Eur. polym. J.*, **32,** 147.
[13] GALLOT, B., MONNET, F., and SIYUAN HE, 1995, *Liq. Cryst.*, **19,** 501.
[14] GALLOT, B., and LENCLUD, A.-L., 1997, *Polymer*, **14,** 3493.
[15] GALLOT, B., LENCLUD, A.-L., and SIYUAN, HE, 1997, *J. appl. polym. Sci.*, **65,** 2407.
[16] *International Tables for X-ray Crystallography, 1*, 1952 (Birmingham: The Kynoch Press).
[17] NEISES, B., and STIEGLISH, W., 1978, *Angew. Chem. int. Ed. Engl.*, **17,** 522.
[18] HOFLE, G., STIEGLISH, W., and VORBRUGGEN, H., 1978, *Angew. Chem. int. Ed. Engl.*, **17,** 569.
[19] DE VRIES, A., 1985, *Mol. Cryst. liq. Cryst.*, **131,** 125.
[20] GUDKOV, V. A., 1984, *Sov. Phys. Crystallog.*, **29,** 316.
[21] ALLIA, P., CUCINELLI, C., PONTI, S., TAVERNA, P., TROSSI, L., and GALLOT, B., 2002, *Liq. Cryst.*, **29,** 405–411.